# Structural and Mechanical Characterization of Crosslinked and Sterilised Nanocellulose-Based Hydrogels for Cartilage Tissue Engineering

‡Ayesha Al-Sabah[a], ‡Stephanie EA Burnell[a], ‡Irina N Simoes[a], Zita Jessop[a,b], Nafiseh Badiei[c], Emma Blain[d] and *Iain S Whitaker[a,b]

[a]Reconstructive Surgery & Regenerative Medicine Group (ReconRegen), Institute of Life Sciences, Swansea University Medical School, SA2 8PP, Swansea, Wales, UK, [b]The Welsh Centre for Burns and Plastic Surgery, Morriston Hospital, SA6 6NL, Swansea, Wales, UK, [c]NanoHealth Centre, Institute of Life Sciences, Swansea University Medical School, SA2 8QA, Swansea, Wales, UK, [d]Arthritis Research UK Biomechanics and Bioengineering Centre, School of Biosciences, Cardiff University, CF10, 3AX, Cardiff, Wales, UK

Ayesha Al-Sabah: aishaalsabah@yahoo.com, Stephanie EA Burnell: stephb90@hotmail.co.uk, Irina N Simoes: irina.nevessimoes@swansea.ac.uk, Zita Jessop: z.m.jessop@swansea.ac.uk, Nafiseh Badiei: n.badiei@swansea.ac.uk, Emma Blain: blain@cardiff.ac.uk and Iain S Whitaker: iainwhitaker@fastmail.fm.

‡Equivalent contributors

**Corresponding author:**

Professor Iain S. Whitaker

Reconstructive Surgery & Regenerative Medicine Group (ReconRegen)

Institute of Life Sciences 2, Swansea University Medical School

Swansea, SA2 8PP, Wales, United Kingdom

Telephone: +44 1792 606311

Fax: +44 1792 703875

E-mail: iainwhitaker@fastmail.fm

## Abstract

Nanocellulose is a natural biopolymer derived from cellulose. Combined with sodium alginate, it is used to 3D print hydrogels for articular and nasal cartilage engineering and shows good integration, promising cartilage regeneration and mechanical stability over 60 days of implantation in mice. Yet, little is known about their structural and mechanical properties, particularly the impact of crosslinking and sterilisation methods. This study investigates the impact of different calcium chloride crosslinker concentrations and sterilization methods on the structural and mechanical properties of nanocellulose-based hydrogels containing plant-derived cellulose nanofibrils, cellulose nanocrystals or a blend of the two. Crosslinking significantly alters the overall network distribution, surface morphology, pore size and porosity of the hydrogels. Sterilisation has a striking effect on pore size and affects swelling depending on the sterilisation method. The effect of crosslinker and sterilisation on the overall properties of the hydrogels was reliant on the form of nanocellulose that comprised them.

**Keywords:** Nanocellulose, Crosslinking, Sterilisation, Hydrogels, Cartilage Tissue Engineering

## 1. Introduction

Tissue engineering can provide advanced alternatives to the current standard surgical procedures used in the field of cartilage repair and reconstruction. For many years, the cartilage tissue engineering field has explored the use of biomaterials, more specifically hydrogels, to create tissue substitutes (Park & Lee, 2014; Tibbitt & Anseth, 2009; Xiao, Friis, Gehrke, & Detamore, 2013). Hydrogels mimic the native extracellular matrix (ECM) and can be tailored to resemble the native structure and mechanics of the tissues, enhance mass transport and support cell adhesion and protein sequestration (S. Lin, Sangaj, Razafiarison, Zhang, & Varghese, 2011; Tibbitt & Anseth, 2009). Importantly, through techniques such as three-dimensional (3D) bioprinting, these hydrogels can be used as bioinks to create high-resolution 3D structures, with any shape or size, to support cell growth and tissue formation (Mouser *et al.*, 2017). As the use of synthetic materials often leads to infection,

extrusion and foreign body reaction, more natural biomaterials are increasingly explored (Anderson, Rodriguez, & Chang, 2008; Baker, Walsh, Schwartz, & Boyan, 2012).

Alginate is a natural and abundant polysaccharide that occurs in marine brown algae and other sources (Hecht & Srebnik, 2016). Water-soluble sodium alginate ($(NaC_6H_7O_6)_n$), the sodium salt of alginic acid, is commonly used as a component of hydrogels for cartilage engineering due to its recognized chondrogenicity and ability to enhance the structural properties of hydrogels (Ansari *et al.*, 2017; Chou, Akintoye, & Nicoll, 2009; Markstedt *et al.*, 2015; Miao *et al.*, 2017).

Within the past decade, nanocellulose (NC) was appointed as an exciting novel biomaterial for biomedical applications due to its attractive physicochemical properties, abundance, sustainability, non-cytotoxicity and biodegradability (Dumanli, 2016; N. Lin & Dufresne, 2014). NC is a biopolymer derived from cellulose, a polysaccharide composed by D-glucopyranose linked by β-1,4 glycosidic bonds (Endes *et al.*, 2016) that is the most abundant, renewable and natural resource available (Dumanli, 2016; N. Lin & Dufresne, 2014). Cellulose contains three hydroxyl groups (-OH) at C-2, C-3 and C-6 positions which determine its physical properties. NC can be found in plants and marine animals and is naturally available in two forms: nanofibrils and nanocrystals (N. Lin & Dufresne, 2014). Additionally, NC is biotechnologically produced in bacteria (N. Lin & Dufresne, 2014). Although the cellulose molecular backbone is common to all forms of NC, the surface morphology, size, chemical and physical properties can vary depending on the material source and extraction methods (Mao *et al.*, 2017). Cellulose nanofibrils and nanocrystals are produced through several chemical, mechanical and/or enzymatic methods that introduce functional groups in the surface of the NC (Kim & Song, 2015). Yet, NC produced through the American Value Added Pulping (AVAP®) technology chemically pre-treats wood-pulp derived biomass and produces NC that is free from any additional functional groups, apart from the -OH groups (Kyle *et al.*, 2018). Importantly, the lack of post-hydrolysis modifications allows facile surface functionalization of the hydroxyl groups resulting in promising potential for novel, advanced and multifunctional biomaterials with improved biocompatibility and tissue generation (Bodin *et al.*, 2007). Bacterial NC can be produced

with high purity and has shown promise for tissue engineering applications (water-holding capacity, mechanical strength and morphological similarities with collagen) and 3D bioprinting (good rheological properties) (Ahrem *et al.*, 2014; Markstedt *et al.*, 2015; Paakko *et al.*, 2007). Yet, the use of bacterial NC for large scale commercialization is limited by the high cost of substrates, low productivity of strains and expensive culture media (Paakko *et al.*, 2007; Revin, Liyaskina, Nazarkina, Bogatyreva, & Shchankin, 2018). Despite the efforts to increase productivity and decrease costs using various waste-products, the production of bacterial NC is still far from large-scale commercialisation and needs further development (Revin *et al.*, 2018). Additionally, there are still concerns regarding residual bacterial toxins/epitopes in bacterial NC (Paakko *et al.*, 2007).

The combination of crosslinked sodium alginate and NC has been recently explored for cartilage tissue engineering, for articular and nasal reconstruction (Ahrem *et al.*, 2014; Martínez Ávila *et al.*, 2015; Möller *et al.*, 2017; Müller, Öztürk, Arlov, Gatenholm, & Zenobi-Wong, 2016; Nguyen *et al.*, 2017). The chondrogenic potential and biocompatibility of these composite hydrogels was reported in both *in vitro* and *in vivo* studies using bacterial NC (Ahrem *et al.*, 2014; Martínez Ávila *et al.*, 2015; Möller *et al.*, 2017; Müller *et al.*, 2016; Nguyen *et al.*, 2017; Svensson *et al.*, 2005). Recently, Müller and colleagues used 3D bioprinted alginate-NC hydrogels and articular bovine chondrocytes to demonstrate high cell viability, proliferation and high collagen type II deposition after 28 days in culture (Müller *et al.*, 2016). Similarly, Nguyen *et al.* reported, using the same composite hydrogels as a scaffold for the differentiation of human induced pluripotent stem (iPS) cells, significant increase in RNA expression of chondrogenic markers and matrix deposition. This increase was confirmed by histology staining and immunohistochemistry upon 5 weeks of differentiation (Nguyen *et al.*, 2017). In 2015, Martínez-Avila and his team reported *in vivo* neocartilage formation using co-cultures of human nasoseptal chondrocytes and bone marrow mononuclear cells in bilayer alginate-NC hydrogels (Martínez Ávila *et al.*, 2015). Briefly, the constructs were implanted subcutaneously in nude mice showing non-pathological foreign body reaction, deposition of proteoglycans and collagen

type II and increased instantaneous modulus upon 8 weeks of implantation (Martínez Ávila *et al.*, 2015).

In these composite hydrogels, sodium alginate provides structural integrity through chemical crosslinking promoting the transition of the hydrogel into a solid material (Caliari & Burdick, 2016). Sodium alginate can be ionically crosslinked by adding calcium ions (crosslinker) which substitute the sodium ions in the alginate, creating strong bonds between alginate chains and ultimately creating a mesh (Hecht & Srebnik, 2016). The concentration of crosslinker can regulate the characteristics of the solid material by tailoring its structural and mechanical properties (S. Lin *et al.*, 2011). Such changes affect the network mesh distribution and pore size that ultimately impact cellular phenotype, proliferation and ECM production (Bryant, Chowdhury, Lee, Bader, & Anseth, 2004; Hwang *et al.*, 2007; Lien, Ko, & Huang, 2009; Villanueva, Klement, von Deutsch, & Bryant, 2009). In cartilage engineering, this has a particularly significant impact on mass transport and the spatial distribution of the ECM – increased hydrogel mesh size leads to higher collagen content, for example (Bryant & Anseth, 2002; Buxton *et al.*, 2007; Chung, Mesa, Randolph, Yaremchuk, & Burdick, 2006; S. Lin *et al.*, 2011). Apart from the extensive body of literature reporting on the chondrogenicity of hydrogels combining sodium alginate and NC, the detailed microenvironment and mechanical properties of these hydrogels remains fairly unknown (Leppiniemi *et al.*, 2017; Markstedt *et al.*, 2015; Martínez Ávila *et al.*, 2015; Müller *et al.*, 2016; Nguyen *et al.*, 2017). Moreover, prior to any application, these hydrogels require sterilisation to limit or prevent the risk of contamination, infection and rejection (Matthews, Gibson, & Samuel, 1994; Veerachamy, Yarlagadda, Manivasagam, & Yarlagadda, 2014). Despite the importance of this topic, less than 1% of the scientific publications in the past decade have focused on the sterilisation methods of hydrogel-based biomedical systems (Galante, Pinto, Colaco, & Serro, 2017). Along with this trend, the effect of sterilisation on the intrinsic properties of NC-based hydrogels also remains elusive. Few studies have performed side-by-side comparison of the architecture, structure and mechanics of the different forms of NC-based hydrogels. Plant-derived

cellulose nanofibrils, cellulose nanocrystals and blend, produced using AVAP® technology have been thoroughly characterised without additives or crosslinking by Kyle *et al.* in 2018 (Kyle *et al.*, 2018). The first aim was to investigate the effect of crosslinking – using calcium chloride ($CaCl_2$) – on the structural and mechanical properties of AVAP® produced plant-derived cellulose nanofibrils, cellulose nanocrystals and blend (combination of nanofibrils and nanocrystals) NC-based hydrogels combined with sodium alginate. Inspired by the hydrogels described in the literature, NC-based hydrogels were crosslinked using increasing concentrations of crosslinker to understand its impact on the overall architecture and characteristic properties (Ahrem *et al.*, 2014; Martínez Ávila *et al.*, 2015; Möller *et al.*, 2017; Müller *et al.*, 2016; Nguyen *et al.*, 2017; Svensson *et al.*, 2005). Secondly, the same type of characterisation was performed upon exposure of the NC-based hydrogels to different sterilisation methods: exposure to ultraviolet (UV) light, autoclaving and ethanol immersion. Finally, the characteristics of the microenvironment of NC-based hydrogels used herein was compared with the reported "ideal" conventional environment for cartilage engineering (Nava, Draghi, Giordano, & Pietrabissa, 2016; Oh, Kim, Im, & Lee, 2010; Pan *et al.*, 2015).

## 2. Hypothesis

The concentration of crosslinker and the sterilisation methods affect the structural and mechanical properties (i.e. pore size, overall network organisation, swelling, porosity and elastic modulus) of NC-based hydrogels.

## 3. Material and Methods

All reagents were purchased from Sigma-Aldrich® (Dorset, UK) unless stated otherwise. All reagents were of analytical grade or above.

### 3.1 Preparation of nanocellulose-based hydrogels

Plant-derived nanocellulose (hydrophilic Bioplus® cellulose nanofibrils gel, hydrophilic Bioplus® cellulose nanocrystals gel and hydrophilic Bioplus® blend gel – a blend of fibrils and crystal) was

155 provided by American Process, Inc. (Georgia, USA) (Kyle *et al.*, 2018). All nanocellulose forms are
156 produced via the AVAP® technology (Kyle *et al.*, 2018) which fractionates biomass into cellulose,
157 hemicelluloses and lignin using ethanol and sulfur dioxide (Kyle *et al.*, 2018). The final nanocellulose
158 product morphology – fibrils (3 wt.% solids), crystals (6 wt.% solids) and blend (3 wt.% solids) was
159 controlled by the time and temperature of the pre-treatment step (Kyle *et al.*, 2018). The blend
160 nanocellulose is produced *in situ* during production and is not an actual blend of fibrils and crystal,
161 yet for simplicity it will be referred to as blend. Hydrogels were prepared by mixing nanocellulose
162 with 2.5% (w/v) sodium alginate (alginic acid sodium salt, from brown algae, 80,000-120,000 Da,
163 medium viscosity (2% at 25ºC), 1.56 mannuronate/guluronate ratio) solution in ultrapure water.
164 Briefly, nanocellulose was centrifuged at 1500 g for 5 min, excess water was removed, and 2.5%
165 sodium alginate solution was added in a 1:4 proportion (Markstedt *et al.*, 2015). NC-based hydrogels
166 were named as follows: NC-blend and 2.5% sodium alginate (NCB), NC-fibrils and 2.5% sodium
167 alginate (CNF) and NC-crystals and 2.5% sodium alginate (CNC). All NC-based hydrogels contained
168 75% of NC, where CNF and NCB had a final concentration of 2.25 wt.% solids and CNC contained
169 4.5 wt.% solids.

170 **3.2 Crosslinking of nanocellulose-based hydrogels**

171 Nanocellulose-based hydrogels were shaped into: (a) 1.5 ml discs (Ø=~14mm) for mechanical testing
172 and (b) 100 µl pellets for all other assays (Figure 1A). The discs were produced using 24 well plates
173 (Cellstar®) and the pellets were produced using 1ml syringes (BD Biosciences©, Oxford, UK) and
174 the indentations of a 96 well plate lid (Cellstar®) as a mould. Crosslinking was performed at room
175 temperature using 0.1 M, 0.5 M or 1.0 M calcium chloride ($CaCl_2$) solutions prepared in ultrapure
176 water. Hydrogels of 2.5% sodium alginate were also prepared as mentioned above. The experimental
177 layout is depicted in Figure 1B.

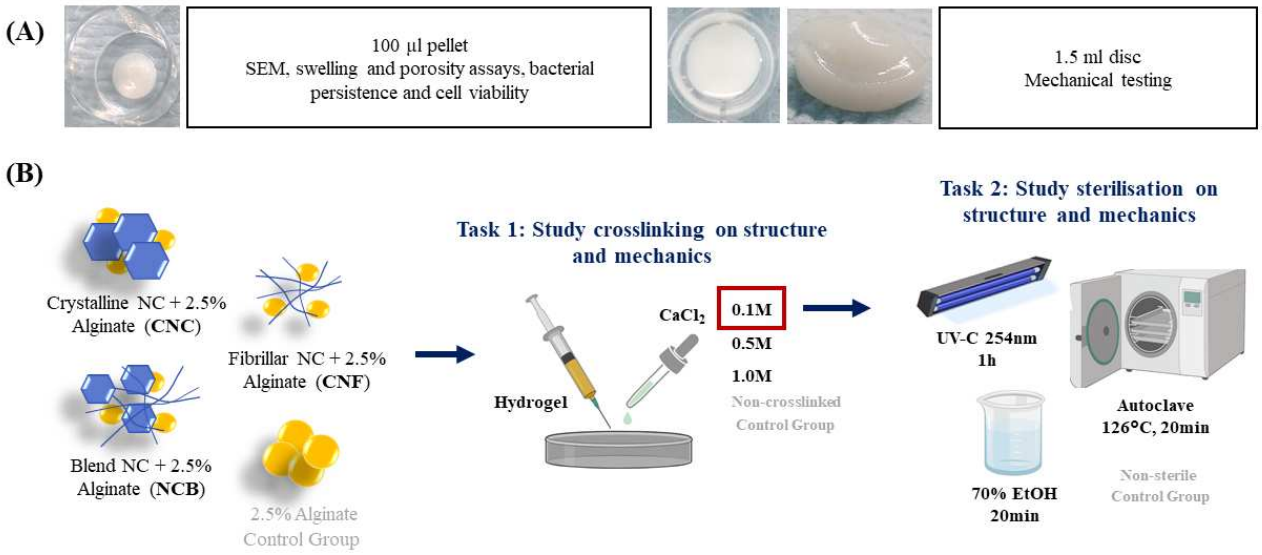


**Figure 1.** Graphical experimental layout. (A) Overall aspect of NC-based hydrogels (pellets and discs). Photos are from NCB-based crosslinked hydrogels. (B) Experimental layout: different NC-based hydrogels were crosslinked with varying concentrations of $CaCl_2$ – structural and mechanical properties were assessed post-crosslinking; NC-based hydrogels crosslinked with the least concentrated $CaCl_2$ solution were subjected to different sterilisation methods – structural and mechanical properties were assessed post-sterilisation. Sodium alginate hydrogels were used as controls in all experiments. NCB – nanocellulose blend of fibrils and crystal; CNC – nanocellulose crystal; CNF – nanocellulose fibrils; $CaCl_2$ – calcium chloride. Image partially created with BioRender©.

### 3.3 Sterilization of nanocellulose-based hydrogels

Nanocellulose-based hydrogels were sterilised using (a) autoclave, (b) UV light (UV-C germicidal light) or (c) ethanol (70% absolute ethanol in ultrapure water). Autoclave sterilisation was performed for 20 min at 126°C using a Classic bench-size autoclave (Prestige Medical, Blackburn, UK). UV sterilisation was completed in petri dishes inside a laminar flow hood using UV-C 254 nm for 1 hour. After sterilisation, hydrogels were crosslinked using 0.1 M $CaCl_2$. Ethanol sterilisation was carried out by immersion of nanocellulose-based hydrogels in ethanol for 20 min – the crosslinking was performed in tandem (*i.e.* the $CaCl_2$ was dissolved in 70% ethanol). Sodium alginate hydrogels were also processed as mentioned above. The experimental layout is depicted in Figure 1B.

### 3.4 Scanning electron microscopy and average pore size calculation

Hydrogels were washed with 50 mM sodium cacodylate-HCl buffer solution (pH 7.2-7.4, SPI Supplies®, West Chester, PA, USA) for 10-20 min, fixed overnight in 2% glutaraldehyde and

dehydrated using a series of graded ethanol concentrations (30%-100%). These were subsequently rinsed with 50% hexamethyldisilazane solution (HMDS) in 100% ethanol for 10 min, then in 100% HMDS and left overnight to dry. The specimens were coated with a thin layer of gold (~15 nm) using sputter coating and examined using scanning electron microscopy (SEM, Hitachi 4800, Hitachi, Schamumburg, IL, USA). Pore size was determined using ImageJ 1.51 software from the National Institutes of Health, USA.

### 3.5 Swelling and porosity assays

Pellets were immersed in 1x PBS (Gibco®, ThermoFisher Scientific, Loughborough, UK) and incubated at 37°C for 24 hours. After blotting the excess PBS on the surface, each pellet was weighed individually ($M_w$). After drying for 48h at room temperature (using desiccant inside a Styrofoam box), the pellets were again weighed individually ($M_d$). Swelling and porosity percentages (%) were given by the Equation 1 and 2 (Caliari & Burdick, 2016; Gupta & Shivakumar, 2012; K. Pal, 2009). PBS density was considered as 1.06 g $cm^{-3}$.

$$Swelling\ \% = \frac{M_w - M_d}{M_d}\ x\ 100 \qquad \text{Equation 1}$$

$$Porosity\ \% = \frac{(M_w - M_d)}{\rho_{PBS}\ x\ V_{pellet}}\ x\ 100 \qquad \text{Equation 2}$$

### 3.6 Mechanical testing

Mechanical tests were performed on wet discs at room temperature using a Bose Electroforce® 3200 (Bose Corp., TA Instruments, MN, USA) equipped with a compression plate. Compressive loading was applied using a 1 Hz frequency at 5 N for 20 cycles. Young's modulus was given by Equation 3, 4, and 5.

$$Young's\ Modulus\ (kPa) = \frac{Stress\ (N\ m^{-2})}{Strain\ (\%)} \qquad \text{Equation 3}$$

Where,

$$Stress = \frac{Force\ (N)}{Area\ (m^2)} \qquad \text{Equation 4}$$

$$Strain = \frac{Length_{pre-load}\ (m) - Length_{post-load}\ (m)}{Length_{pre-load}\ (m)} \qquad \text{Equation 5}$$

The length and surface area were determined pre- and post-loading using a digital calliper.

### 3.7 Bacterial persistence

Bacterial persistence post-sterilisation was determined through optical density (OD) at 600 nm using a spectrophotometer. Samples were horizontally and vertically cut into four equal pieces with similar exposed surface area and added to a tube containing 10 ml of lysogeny broth (LB). After 24h and 48h at 37°C under constant stirring, 1ml samples were taken out and used to measure OD.

### 3.8 Cell viability

Human naso-septal chondrocytes were isolated from healthy donors, after informed consent from patients (IRAS ID 99202) at ABM University Health Board, Swansea, United Kingdom. Samples were collected during routine septorhinoplasty procedures where the cartilage would have otherwise been discarded (institutional review committee approved the study, ethics approval: REC 12/WA/0029), following an adjusted protocol (Dowthwaite *et al.*, 2004; Fickert, Fiedler, & Brenner, 2004). Cells were extracted overnight using 2.0 mg $ml^{-1}$ pronase and 2.4 mg $ml^{-1}$ collagenase I and cultured in DMEM with 10% fetal bovine serum (FBS), 1% penicillin-streptomycin solution, 1mM D-glucose solution and 0.1% minimum essential medium (MEM) non-essential amino acids (all from Gibco®) in a humidified 37°C incubator with 5% $CO_2$. After 2.5 weeks, chondrocytes were mixed with the sterilised hydrogels (3 x $10^5$ cells per pellet) to prepare 100 µl pellets, as mentioned previously, and crosslinked using 0.1 M $CaCl_2$. Pellets were cultured for up to 7 days – cell viability was determined at 24h and 7 days using Live/Dead assay kit (ThermoFisher Scientific) according to manufacturer's instructions. The pellets were imaged using confocal microscopy (Zeiss 710 confocal microscope, Zeiss, Cambridge, UK) and ZEN software (Zeiss).

### 3.9 Statistical analysis

Data are expressed as mean ± standard error of the mean (mean ± SEM). All data were checked for normality (Anderson-Darling Test) and equal variance (Levene's Test) to meet the assumptions of ANOVA. An ANOVA followed by a Tukey test for *post-hoc* pairwise comparisons were used.

Alternatively, Mann-Whitney U tests were used for data with unequal variance. Statistical analysis was performed using Minitab® 18 (Minitab Inc.). A p-value < 0.05 was considered significant.

## 4. Results and Discussion

In recent years, NC-based hydrogels have been used for cartilage engineering purposes providing promising *in vitro* and *in vivo* outcomes (Martínez Ávila *et al.*, 2015; Nguyen *et al.*, 2017). However, little is known about the effects of crosslinking concentrations and sterilisation methods on the hydrogel structure, microarchitecture, and mechanical properties. If these hydrogels are to be translated to clinic, it is essential to understand how such processing methods affect their properties. In this study, we initially looked at the effect of increasing crosslinker concentrations and later investigated the impact of different sterilisation methods. NC-based hydrogels possess excellent rheological properties for applications such as 3D bioprinting, however these must be supplemented with a biomaterial that enables crosslinking to ensure post-printing shape fidelity (Kyle et al., 2018). To that end, we used plant-derived cellulose nanofibrils, cellulose nanocrystals and a blend, produced via the AVAP® technology which do not crosslink on their own when exposed to various concentrations of $CaCl_2$ (data not shown). Sodium alginate was used to provide structural integrity via ionic crosslinking using $CaCl_2$ (Hecht & Srebnik, 2016). NC-based hydrogels were formulated by mixing sodium alginate and different NC forms: crystalline (CNC), fibrillar (CNF) and blend (NCB) (Figure 1 and Supplementary Material, Figure S1). The surface charge of the different NC forms were previously evaluated by means of the zeta potential (Kyle *et al.*, 2018). All NC forms showed negative zeta potential in neutral water. As such, this feature was dismissed for the discussion as it would not explain structural and mechanical differences between the composite hydrogels.

### 4.1 Characterization of crosslinked NC-based hydrogels

The surface morphology and network distribution of the different NC-based hydrogels were observed through SEM images (Figure 2A-P). CNC and CNF showed different surface morphologies – CNF contains a fibrillar-like network with varying thickness (Figure 2I) while CNC holds a leaf-like net

architecture (Figure 2M). The overall surface morphology of NCB, a blend of CNC and CNF, is apparently more porous and interconnected than CNF and CNC individually (Figure 2E). Upon addition of the crosslinker, the overall structural morphology and network distribution change noticeably. Increasing concentrations of $CaCl_2$ developed a denser and more organised network in the sodium alginate hydrogels, creating an apparent flatter external surface (Figure 2A-D). In the NC-based hydrogels the same trend was observed, although visible differences were more obvious when comparing the highest $CaCl_2$ concentration (Figure 2H, 2L and 2P) with the other two concentrations (Figure 2F-G, 2J-K and 2N-O). As sodium alginate is the structural crosslinked component of the NC-based hydrogels, the NC is in the interstitial framework of sodium alginate and thus seems relatively disorganised, making these changes only noticeable at higher crosslinker concentration. With increasing $CaCl_2$, the gelation rate increases as it is directly proportional to the concentration of calcium ions (Lee & Rogers, 2012). The resulting hydrogel has increased interactions between sodium alginate chains, as additional binding sites on alginate become occupied by calcium ions (Fang *et al.*, 2007). The network of NC-based hydrogels is moderately different between NCB, CNC and CNF, yet noticeably different from the sodium alginate hydrogels: alginate has a more organised and uniform pore distribution whereas NC-based hydrogels are more irregular with varying pore distribution and pore interconnectivity. These findings are related to the structural organisation of sodium alginate as linear unbranched chains – the differences observed are more prominent due to a higher level of organisation of alginate when compared to NC-based hydrogels (Vold, Kristiansen, & Christensen, 2006). Average pore size was confirmed through ImageJ measurements (Figure 2Q), showing significant differences ($p<0.05$) in all hydrogels when exposed to the crosslinker. The impact of different $CaCl_2$ concentrations on pore size was particularly accentuated in the sodium alginate hydrogels ($p<0.0001$), confirming the tendency observed through SEM (Figure 2A-D). Interestingly, CNC exposed to the lowest $CaCl_2$ concentration had smaller pores than the ones subjected to the highest concentration ($0.68 \pm 0.05$ µm versus $0.84 \pm 0.08$ µm, respectively, Figure 2Q). The lower porosity along higher crosslinking concentrations is due to the enhanced association of sodium

alginate polymers inadvertently reducing porosity (Peretz *et al.*, 2014) – more crosslinker particles translates into more bonds between the α-L-guluronic chains of sodium alginate (Hecht & Srebnik, 2016). CNF showed the same trend as CNC, although a significant decrease ($p<0.05$) was seen between 0.5M $CaCl_2$ and 1.0M $CaCl_2$ (Figure 2Q). Contrarily, the NCB crosslinked with 1.0M $CaCl_2$ showed smaller pore sizes than the ones exposed to lower concentrations (0.61 ± 0.05 µm versus 0.87 ± 0.09 µm and 0.86 ± 0.07 µm, respectively, Figure 2Q). A similar trend was observed when evaluating average pore size at a higher magnification (Supplementary Material, Figure S2A). The differences seen in NC-based hydrogels are possibly due to the diluted sodium alginate polymers tight interaction, but the presence of NC in between the chains prevents the formation of a tighter and organised network as observed with sodium alginate on its own.

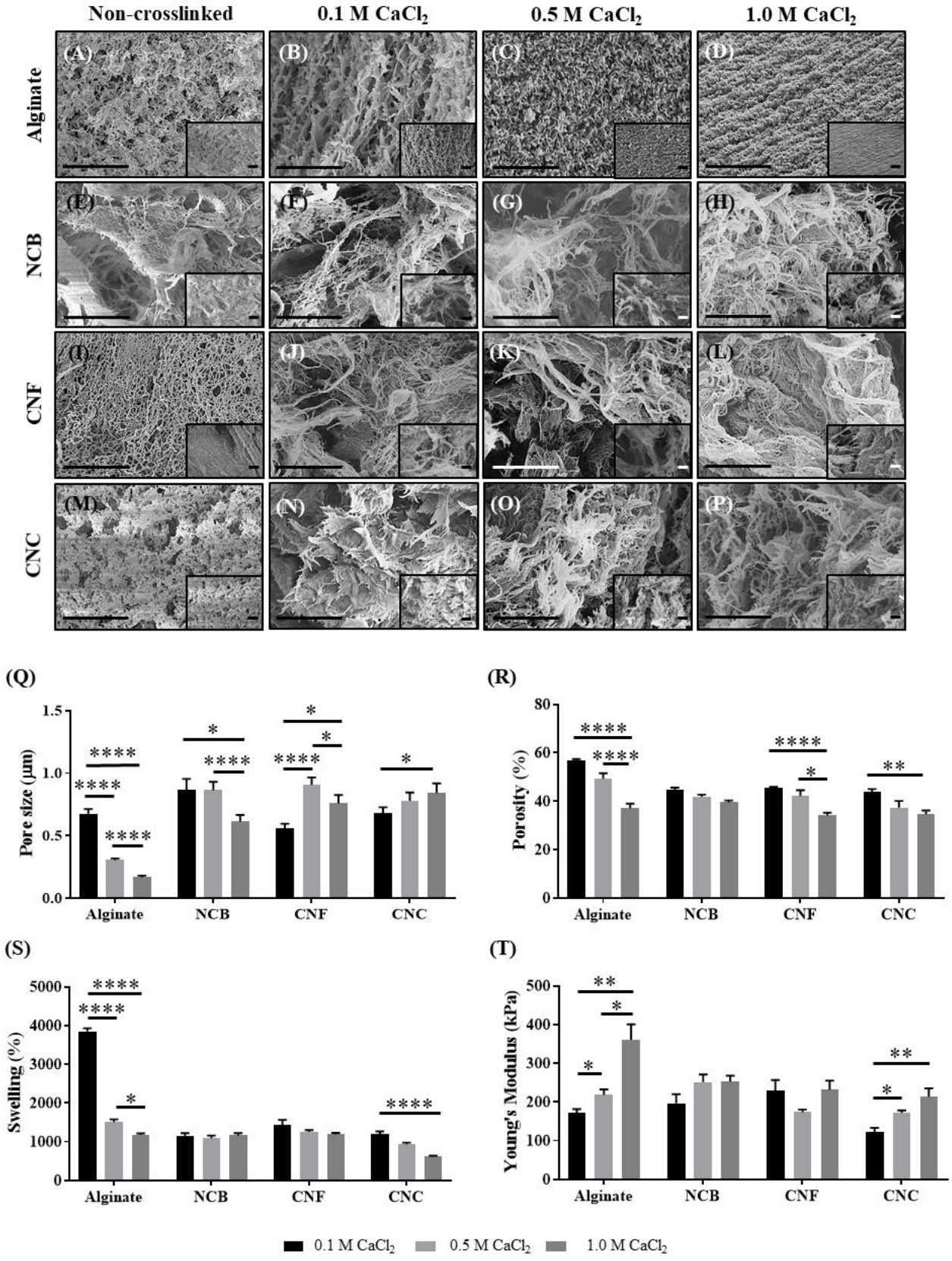


309

310 **Figure 2.** Structure and mechanics of NC-based hydrogels post-crosslinking with different $CaCl_2$ concentrations. (A-P)
311 Overall network architecture and pore distribution. Images taken at 9k and 20k magnifications. Scale bar = 2 µm. (Q)
312 Average pore size (µm) post-crosslinking based on 9k magnification SEM images. Mean ± SEM, n=80 measurements.

(R) Porosity and (S) swelling percentages post-crosslinking. Mean ± SEM, n=6. (T) Young's modulus (kPa) based on compression post-crosslinking. Mean ± SEM, n=6. NCB – nanocellulose blend; CNC – nanocellulose crystal; CNF – nanocellulose fibrils; $CaCl_2$ – calcium chloride; 0.1M $CaCl_2$ – black; 0.5M $CaCl_2$ – light grey; 1.0M $CaCl_2$ – grey. Mann Whitney (Q and T) and ANOVA (R and S) statistical tests: *, $p \leq 0.05$; **, $p \leq 0.01$; ****, $p \leq 0.0001$.

The overall porosity of NCB was not affected by the concentration of the crosslinker ($p>0.05$, Figure 2R). In all other hydrogels, the porosity decrease was more accentuated between the lowest and the highest $CaCl_2$ concentrations: sodium alginate (56.7 ± 0.8% versus 37.2 ± 1.9%, $p<0.0001$), CNF (45.6 ± 0.3% versus 34.2 ± 1.0%, $p<0.0001$) and CNC (43.7 ± 1.4% versus 34.6 ± 1.60%, $p<0.01$) (Figure 2R). The swelling capacity of NCB and CNF was not affected by the crosslinker concentration (Figure 2S). Conversely, the swelling of sodium alginate and CNC was affected by $CaCl_2$ concentration – swelling decreased to at least half when exposed to 1.0M $CaCl_2$ ($p<0.0001$, Figure 2S). Overall, in NC-based hydrogels, the use of 0.5M $CaCl_2$ showed milder effects for both porosity and swelling percentages (Figures 2R and 2S). Finally, the stiffness of the crosslinked hydrogels was measured based on Young's Modulus (Figure 2T). NCB and CNF retained similar stiffness independent of the crosslinker concentration ($p>0.05$, Figure 2T). However, CNC and sodium alginate yielded stiffer hydrogels when exposed to higher $CaCl_2$ concentrations (Figure 2T). These similarities may be related to the ordered structural organisation of both sodium alginate and CNC (Ma *et al.*, 2017). The sodium alginate crosslinked with 1.0M $CaCl_2$ produced the stiffest hydrogel tested (361 ± 40 kPa, Figure 2T).

Overall, the effect of crosslinker is more striking in sodium alginate hydrogels than NC-based hydrogels. Among the different NC forms, CNC seems to be the most affected by varying crosslinker concentrations while NCB retains most of its characteristics independent of crosslinker concentrations.

### 4.2 Characterization of sterilised NC-based hydrogels

The use of low crosslinker concentrations has been widely demonstrated as the optimal crosslinking method as it promotes a slower gelation rate, uniform structure, and enhanced mechanical integrity

(Kuo & Ma, 2001; Skjåk-Bræk, Grasdalen, & Smidsrød, 1989). As a result, 0.1M $CaCl_2$ was used to assess the effects of the various sterilisation methods on sodium alginate and NC-based hydrogels. Due to the temperature sensitive nature of sodium alginate, autoclave sterilisation was not pursued as the high temperatures promote depolymerisation of alginate (Leo, Mcloughlin, & Malone, 1990). Changes in the surface morphology and network distribution in the different NC-based hydrogels upon sterilisation was confirmed through SEM (Figure 3A-P). All sterilisation methods showed an apparent impact on the overall network distribution. The most striking differences were observed in sodium alginate hydrogels when exposed to any sterilisation method (Figure 3A-D). Both UV and ethanol sterilisations transformed the network of the NC-based hydrogels into a more leaf-like architecture while autoclave seemed to accentuate the fibrillar features of the network (Figure 3E-P). No visible network differences were observed between different NC-based hydrogels exposed to the same sterilisation method. Sterilisation significantly decreased the average pore size of all hydrogels by 17% – 86 % ($p<0.0001$, Figure 3Q), which is similarly seen in sterilisation of silk-fibroin hydrogels in other studies (Hofmann, Stok, Kohler, Meinel, & Müller, 2014). Autoclave sterilisation resulted in hydrogels with the largest pore size – a trend that was observed in all tested hydrogels (Figure 3Q). Heat sterilisation using the autoclave process replaces the air in the container, creating pressure and leading to the formation of larger pores. Similar trends were observed when evaluating average pore size at a higher magnification (Supplementary Material, Figure S2B). UV and ethanol sterilisations have shown roughly similar pore sizes in all NC-based hydrogels however, the porosity was not affected. This might be related to the rearrangement and fragmentation of the pores during sterilisation, resulting in smaller pores but no changes in overall porosity. This is evident when examining the swelling percentage of NC-based hydrogels. Apart from the alterations in average pore size post-sterilisation, the overall porosity was maintained in all hydrogels except for sodium alginate, where ethanol significantly decreased overall porosity by ~6% ($p<0.05$, Figure 3R). The swelling capacity of sodium alginate hydrogels decreased significantly post-UV ($p<0.05$) and post-ethanol sterilisation ($p<0.0001$, Figure 3S). However, with regards to NC-based hydrogels there was an

overall increase in swelling capacity post-sterilisation, with UV sterilisation yielding hydrogels with the highest swelling percentage ($p<0.001$, Figure 3S). UV irradiation has sufficient energy to disrupt covalent bonds and result in the formation of free radicals which propagate degradation (Wasikiewicz, Yoshii, Nagasawa, Wach, & Mitomo, 2005). The results suggest that UV treatment potentiated the formation of smaller pores which enhanced the swelling potential of all NC-based hydrogels. This is corroborated by the pore size measurements of UV treated NC-based hydrogels. Measurements of stiffness post-sterilisation showed that overall ethanol creates hydrogels with a higher Young's modulus (Figure 3T). This trend was significantly higher in sodium alginate (306 ± 32.8 kPa, $p<0.001$), CNF (508 ± 94.5 kPa, $p<0.05$), and CNC (420 ± 62.7 kPa, p<value 0.001) hydrogels. Ethanol is known for its dehydration properties resulting in the compaction of hydrogels – which explains the higher mechanical strength post-sterilisation as the resultant gels are stiffer (Eltoum, Fredenburgh, Myers, & Grizzle, 2001). The two other sterilisation methods showed variable effects on hydrogel stiffness (Figure 3T): autoclave sterilisation significantly reduced the Young's modulus of CNF hydrogels (148 ± 12 kPa, $p<0.05$), whereas it had the opposite effect on CNC hydrogels (173 ± 12.7 kPa, $p<0.05$). Although it has not been reported in the literature, we theorize that UV and autoclave treatments cause the breakage of clusters of CNC within the hydrogel, resulting in an increase in homogeneity which can be observed in the SEM images post-sterilisation. CNF was not degraded by the thermal energy generated from the autoclave, yet the SEM images show that the fibrils have undergone structural alterations, such as fibril realignment, thus resulting in larger pore size post-sterilisation out of all NC-based hydrogels, which translated into weaker mechanical properties (Kyle *et al.*, 2018; Yang, Yan, Chen, Lee, & Zheng, 2007). All sterilisation methods did not significantly affect the stiffness of NCB hydrogels (Figure 3T). In contrast, all the sterilisation methods used affected the stiffness of CNC (UV, 177 ± 6.6 kPa, $p<0.05$; autoclave, 173 ± 12.7 kPa, $p<0.05$; ethanol, 420 ± 62.7 kPa, $p<0.001$, Figure 3T).

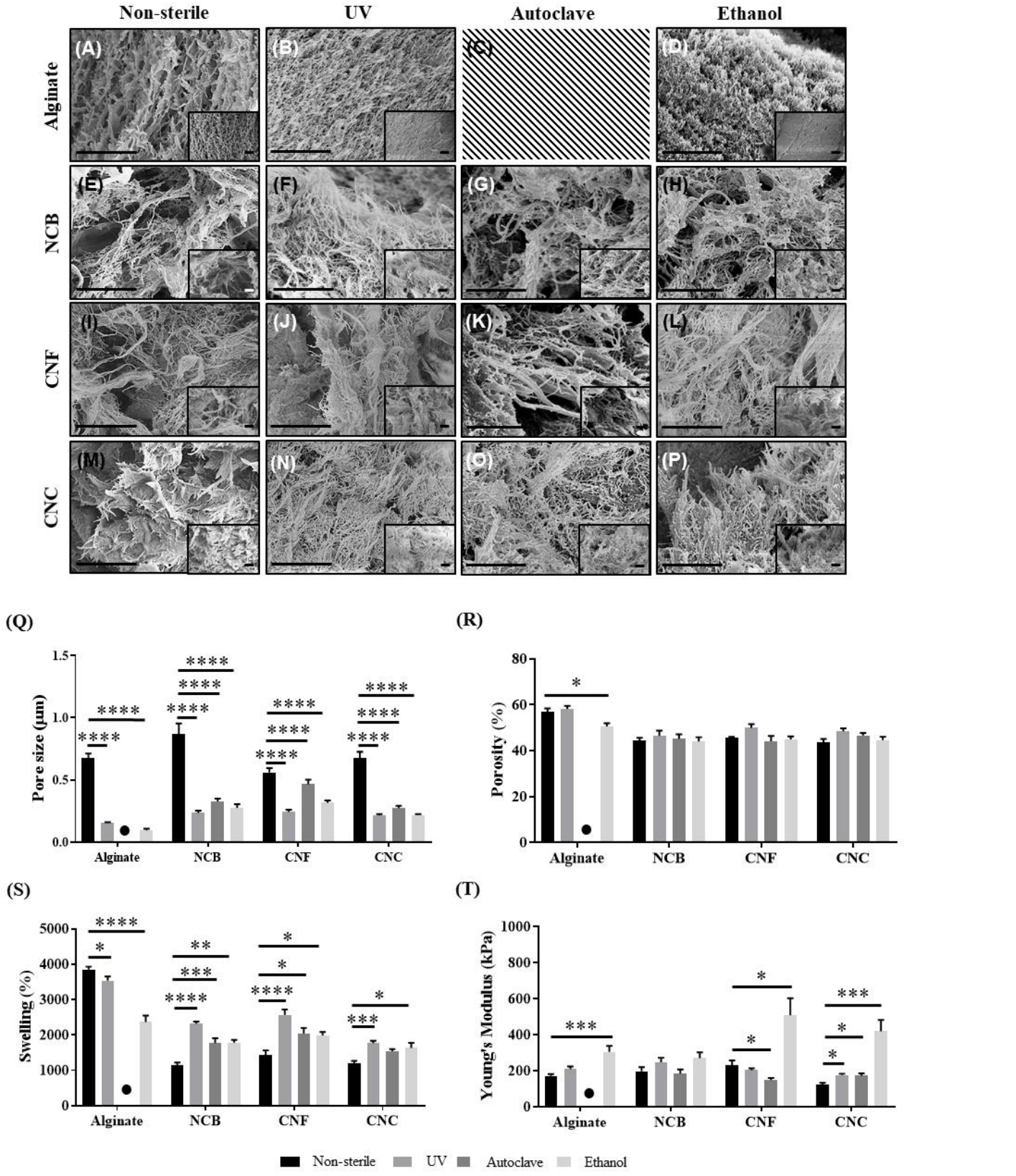


**Figure 3.** Structure and mechanics of NC-based hydrogels post-sterilisation with different methods. (A-P) Overall network architecture and pore distribution. Images taken at 9k and 20k magnification. Scale bar = 2 µm. (Q) Average pore size (µm) post-sterilisation based on 9k magnification SEM images. Mean ± SEM, n=80 measurements. (R) Porosity and (S) swelling percentages post-sterilisation. Mean ± SEM, n=5-6. (T) Young's modulus (kPa) based on compression

post-sterilisation. Mean ± SEM, n=6. NCB – nanocellulose blend; CNC – nanocellulose crystal; CNF – nanocellulose fibrils; Non-sterile – black; UV – grey; Autoclave – dark grey; Ethanol – light grey. ●, absent graph bar: autoclaved sodium alginate hydrogels were not tested. Mann Whitney (Q and T) and ANOVA (R and S) statistical tests: *, $p \leq 0.05$; **, $p \leq 0.01$; ***, $p \leq 0.001$; ****, $p \leq 0.0001$.

### 4.3 Bacterial persistence in sterilised NC-based hydrogels

The efficiency of the sterilisation processes was examined through bacterial persistence (Figure 4). Sterilisation efficiency was evaluated using the respective non-sterile material as a control and all sterilisation methods were confirmed as effective in removing bacterial content. All sterilisation methods showed significant reduction of OD in the hydrogels post-sterilisation ($p<0.05$, Figure 4). Overall, UV sterilisation was the most inefficient method for the sterilisation of NC-based hydrogels (Figure 4). UV sterilisation was very efficient in sodium alginate hydrogels, indicating it is optimal for materials that are transparent – due to its limited penetrability – but not ideal for NC-based hydrogels (Lerouge, 2012). Conversely, the autoclave method was the most efficient for all hydrogels ($p<0.0001$, Figure 4). Although it resulted in structural alterations, it is the optimal method to ensure the elimination of potential contaminants including fungal and bacterial spores (Rogers, 2012). In practice, the use of ethanol is unfeasible as this would result in cell death, as observed in the cell viability tests.

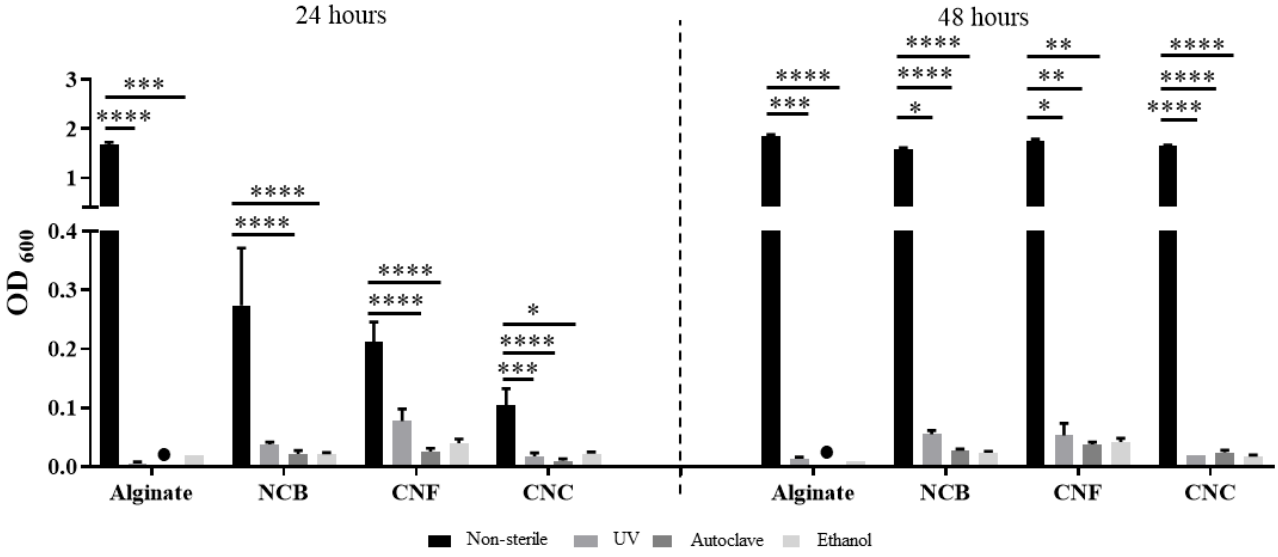


**Figure 4.** Bacterial persistence at 24h and 48h post-sterilisation. Mean ± SEM, n=4-5. NCB – nanocellulose blend; CNC – nanocellulose crystal; CNF – nanocellulose fibrils. Non-sterile – black; UV – grey; Autoclave – dark grey; Ethanol –

light grey. ●, absent graph bar: autoclaved sodium alginate hydrogels were not tested. Mann Whitney statistical test: *, $p \leq 0.05$; **, $p \leq 0.01$; ***, $p \leq 0.001$; ****, $p \leq 0.0001$.

### 4.4 Cell viability assessment using sterilised NC-based hydrogels

Cell viability in the hydrogels was assessed at 1- and 7-days post-sterilisation using human naso-septal chondrocytes and Live/Dead® assay kit (Figure 5 and Supplementary Material, Figure S3). Upon 24h in culture in sterilised hydrogels, cell viability was minimally affected, apart from the cells in ethanol-sterilised hydrogels where most of the cells were dead (Figure 5). After 7 days, the number of dead cells increased in all hydrogels although it was visibly lower than the number of live cells which is indicative of cellular turnover (Supplementary Material, Figure S3). Yet, the low cell viability outcomes in ethanol sterilisation could be related to a limitation of this study – ethanol sterilisation and crosslinking were performed in tandem, meaning that the cells were exposed to 70% ethanol for 20 min, which resulted in higher cell death when compared to other methods. Technically, for the ethanol sterilisation, it was not possible to sterilise the non-crosslinked NC-based hydrogels with ethanol because the removal of ethanol by centrifugation would result in decreased water content in the hydrogels.

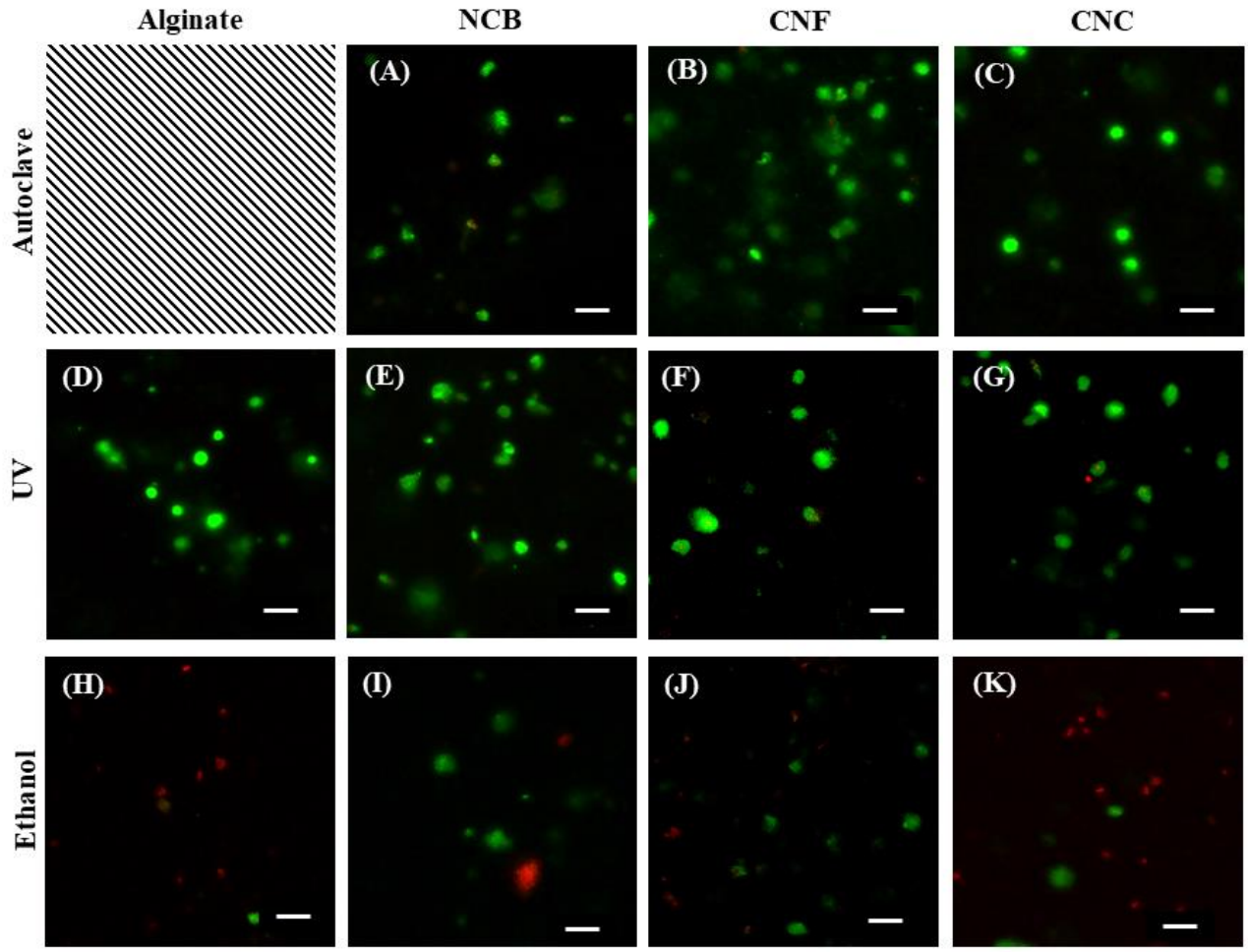


**Figure 5.** Representative cell viability on sterilised hydrogels after 24h under standard culture. Live cells are stained green and dead cells are stained red as assessed using Live/Dead assay kit®. Crossed out panel represents non-tested condition – autoclaved sodium alginate hydrogels. Scale bar = 50 µm.

Importantly, these characterization studies showed that the properties of NC-based hydrogels do not fall under the "conventional" ideal chondrogenic environment described in the literature – 75-400µm pores and 75-97% porosity (Ahrem *et al.*, 2014; Markstedt *et al.*, 2015; Martínez Ávila *et al.*, 2015; Möller *et al.*, 2017; Müller *et al.*, 2016; Nava *et al.*, 2016; Nguyen *et al.*, 2017; Oh *et al.*, 2010; Pan *et al.*, 2015). In general, the NC-based hydrogels had 34-50% porosity and with average pore sizes ranging from 0.22µm to 0.91µm, depending on the NC form assessed. This demonstrates that the definition of ideal environment for cartilage engineering might be broader than expected.

## 5. Conclusion

Previous studies have shown that NC contains favourable properties for diverse biological and medical applications. NC-based hydrogels have been extensively explored for cartilage engineering purposes, mainly using 3D bioprinting technologies.

In this study, composite hydrogels containing sodium alginate and different forms of plant-derived NC (nanocellulose fibrils, nanocellulose crystals or a blend), ionically crosslinked with $CaCl_2$, were shown to have alterations in their structural and mechanical properties upon standard processing methods such as crosslinking and sterilisation. Increasing concentrations of the crosslinker $CaCl_2$ yielded visible changes in overall architecture, pore size (as demonstrated through SEM) and porosity. As sodium alginate crosslinks faster with increasing concentrations of $CaCl_2$, the resulting mesh network will have a different distribution and size, with the different NC forms entrapped in the interstitial areas of the mesh – providing characteristic architectures according their structure (i.e. fibrils or crystals). The swelling capacity and the mechanical properties (as assessed by the Young's Modulus) of the NC-based hydrogels were also affected with increasing crosslinker concentrations, yet not all NC forms were significantly affected.

When exposed to different sterilisation methods (physical, thermal and chemical), the crosslinked NC-based hydrogels showed striking significant decreases in average pore size, while porosity was maintained. From all the properties tested, pore size was the most affected by the sterilisation method, possibly due to the re-arrangement of particles inside the hydrogels. The mechanical properties of the hydrogels were mildly affected by the sterilisation method, apart from the chemical sterilisation using ethanol that yielded significantly stronger hydrogels, possibly due to the dehydration of the hydrogels. Importantly, differential effects were observed based on the NC form contained in the composite hydrogels. Among the NC forms, CNC was more affected by the crosslinker concentrations, CNF and CNC were affected by all sterilization methods with different methods affecting properties differently while NCB was more resilient to changes when exposed to different sterilisation methods and crosslinker concentrations. This indicates that the crosslinking reactions and the sterilisation

method used to process these hydrogels need to be chosen and tailored to the final aim (e.g. tissue type) as these will significantly alter the final environment to which cells will be exposed.

The study of structural and mechanical alterations upon different processing methods is important as it impacts the characteristics of the final product. These will directly affect, for example, its microstructure and microenvironment, ultimately impacting cell phenotype and behaviour when targeting biomedical applications.

## Acknowledgments

This work was supported by Abertawe Bro Morgannwg University (ABMU) Health Board, Health and Care Research Wales, Oakgrove Medical Charitable Trust, the Royal College of Surgeons of England and the Medical Research Council (grant no. MR/N002431/1). We acknowledge the Arthritis Research UK Biomechanics and Bioengineering Centre (Cardiff University) for access to the ElectroForce™ 3200 loading equipment and Mrs. Kavitha Saw for collecting the human naso-septal samples at Singleton Hospital, Swansea, UK. Dr. Ayesha Al-Sabah, Dr. Stephanie EA Burnell, and Dr. Irina N Simoes have equally contributed to this work.

## References

Ahrem, H., Pretzel, D., Endres, M., Conrad, D., Courseau, J., Müller, H., . . . Kinne, R. W. (2014). Laser-structured bacterial nanocellulose hydrogels support ingrowth and differentiation of chondrocytes and show potential as cartilage implants. *Acta Biomaterialia,* 10(3), 1341-1353.

Anderson, J. M., Rodriguez, A., & Chang, D. T. (2008). Foreign body reaction to biomaterials. *Semin Immunol,* 20(2), 86-100.

Ansari, S., Diniz, I. M., Chen, C., Aghaloo, T., Wu, B. M., Shi, S., & Moshaverinia, A. (2017). Alginate/hyaluronic acid hydrogel delivery system characteristics regulate the differentiation of periodontal ligament stem cells toward chondrogenic lineage. *J Mater Sci Mater Med,* 28(10), 162.

Baker, M. I., Walsh, S. P., Schwartz, Z., & Boyan, B. D. (2012). A review of polyvinyl alcohol and its uses in cartilage and orthopedic applications. *J Biomed Mater Res B Appl Biomater,* 100(5), 1451-1457.

Bodin, A., Ahrenstedt, L., Fink, H., Brumer, H., Risberg, B., & Gatenholm, P. (2007). Modification of nanocellulose with a xyloglucan-RGD conjugate enhances adhesion and proliferation of endothelial cells: implications for tissue engineering. *Biomacromolecules,* 8(12), 3697-3704.

Bryant, S. J., & Anseth, K. S. (2002). Hydrogel properties influence ECM production by chondrocytes photoencapsulated in poly(ethylene glycol) hydrogels. *J Biomed Mater Res,* 59(1), 63-72.

Bryant, S. J., Chowdhury, T. T., Lee, D. A., Bader, D. L., & Anseth, K. S. (2004). Crosslinking density influences chondrocyte metabolism in dynamically loaded photocrosslinked poly(ethylene glycol) hydrogels. *Ann Biomed Eng,* 32(3), 407-417.

Buxton, A. N., Zhu, J., Marchant, R., West, J. L., Yoo, J. U., & Johnstone, B. (2007). Design and characterization of poly(ethylene glycol) photopolymerizable semi-interpenetrating networks for chondrogenesis of human mesenchymal stem cells. *Tissue Eng,* 13(10), 2549-2560.

Caliari, S. R., & Burdick, J. A. (2016). A practical guide to hydrogels for cell culture. *Nat Methods,* 13(5), 405-414.

Chou, A. I., Akintoye, S. O., & Nicoll, S. B. (2009). Photo-crosslinked Alginate Hydrogels Support Enhanced Matrix Accumulation by Nucleus Pulposus Cells In Vivo. *Osteoarthritis and cartilage / OARS, Osteoarthritis Research Society,* 17(10), 1377-1384.

Chung, C., Mesa, J., Randolph, M. A., Yaremchuk, M., & Burdick, J. A. (2006). Influence of gel properties on neocartilage formation by auricular chondrocytes photoencapsulated in hyaluronic acid networks. *J Biomed Mater Res A,* 77(3), 518-525.

Dowthwaite, G. P., Bishop, J. C., Redman, S. N., Khan, I. M., Rooney, P., Evans, D. J., . . . Archer, C. W. (2004). The surface of articular cartilage contains a progenitor cell population. *J Cell Sci,* 117(Pt 6), 889-897.

Dumanli, A. G. (2016). Nanocellulose and its Composites for Biomedical Applications. *Curr Med Chem*.

Eltoum, I., Fredenburgh, J., Myers, R. B., & Grizzle, W. E. (2001). Introduction to the Theory and Practice of Fixation of Tissues. *Journal of Histotechnology,* 24(3), 173-190.

Endes, C., Camarero-Espinosa, S., Mueller, S., Foster, E. J., Petri-Fink, A., Rothen-Rutishauser, B., . . . Clift, M. J. D. (2016). A critical review of the current knowledge regarding the biological impact of nanocellulose. *Journal of Nanobiotechnology,* 14.

Fickert, S., Fiedler, J., & Brenner, R. E. (2004). Identification of subpopulations with characteristics of mesenchymal progenitor cells from human osteoarthritic cartilage using triple staining for cell surface markers. *Arthritis Res Ther,* 6(5), R422-432.

Galante, R., Pinto, T. J. A., Colaco, R., & Serro, A. P. (2017). Sterilization of hydrogels for biomedical applications: A review. *J Biomed Mater Res B Appl Biomater*.

Gupta, N. V., & Shivakumar, H. G. (2012). Investigation of Swelling Behavior and Mechanical Properties of a pH-Sensitive Superporous Hydrogel Composite. *Iran J Pharm Res,* 11(2), 481-493.

Hecht, H., & Srebnik, S. (2016). Structural Characterization of Sodium Alginate and Calcium Alginate. *Biomacromolecules,* 17(6), 2160-2167.

Hofmann, S., Stok, K. S., Kohler, T., Meinel, A. J., & Müller, R. (2014). Effect of sterilization on structural and material properties of 3-D silk fibroin scaffolds. *Acta Biomaterialia,* 10(1), 308-317.

Hwang, N. S., Varghese, S., Lee, H. J., Theprungsirikul, P., Canver, A., Sharma, B., & Elisseeff, J. (2007). Response of zonal chondrocytes to extracellular matrix-hydrogels. *FEBS Lett,* 581(22), 4172-4178.

K. Pal, A. K. B., D. K. Majumdar. (2009). Polymeric Hydrogels: Characterization and Biomedical Applications - A mini review. *Designed Monomers and Polymers,* 12, 34.

Kim, D. H., & Song, Y. S. (2015). Rheological behavior of cellulose nanowhisker suspension under magnetic field. *Carbohydr Polym,* 126, 240-247.

Kuo, C. K., & Ma, P. X. (2001). Ionically crosslinked alginate hydrogels as scaffolds for tissue engineering: Part 1. Structure, gelation rate and mechanical properties. *Biomaterials,* 22(6), 511-521.

Kyle, S., Jessop, Z. M., Al-Sabah, A., Hawkins, K., Lewis, A., Maffeis, T., . . . Whitaker, I. S. (2018). Characterization of pulp derived nanocellulose hydrogels using AVAP(R) technology. *Carbohydr Polym,* 198, 270-280.

Leo, W. J., Mcloughlin, A. J., & Malone, D. M. (1990). Effects of Sterilization Treatments on Some Properties of Alginate Solutions and Gels. *Biotechnology Progress,* 6(1), 51-53.

Leppiniemi, J., Lahtinen, P., Paajanen, A., Mahlberg, R., Metsa-Kortelainen, S., Pinomaa, T., . . . Hytonen, V. P. (2017). 3D-Printable Bioactivated Nanocellulose-Alginate Hydrogels. *ACS Appl Mater Interfaces,* 9(26), 21959-21970.

Lerouge, S. (2012). *5 - Non-traditional sterilization techniques for biomaterials and medical devices*. In S. Lerouge & A. Simmons (Eds.), *Sterilisation of Biomaterials and Medical Devices* (pp. 97-116): Woodhead Publishing

Lien, S. M., Ko, L. Y., & Huang, T. J. (2009). Effect of pore size on ECM secretion and cell growth in gelatin scaffold for articular cartilage tissue engineering. *Acta Biomater,* 5(2), 670-679.

Lin, N., & Dufresne, A. (2014). Nanocellulose in biomedicine: Current status and future prospect. *European Polymer Journal,* 59, 24.

Lin, S., Sangaj, N., Razafiarison, T., Zhang, C., & Varghese, S. (2011). Influence of physical properties of biomaterials on cellular behavior. *Pharm Res,* 28(6), 1422-1430.

Ma, X., Li, R., Zhao, X., Ji, Q., Xing, Y., Sunarso, J., & Xia, Y. (2017). Biopolymer composite fibres composed of calcium alginate reinforced with nanocrystalline cellulose. *Composites Part A: Applied Science and Manufacturing,* 96, 155-163.

Mao, Y., Liu, K., Zhan, C., Geng, L., Chu, B., & Hsiao, B. S. (2017). Characterization of Nanocellulose Using Small-Angle Neutron, X-ray, and Dynamic Light Scattering Techniques. *J Phys Chem B,* 121(6), 1340-1351.

Markstedt, K., Mantas, A., Tournier, I., Martínez Ávila, H., Hägg, D., & Gatenholm, P. (2015). 3D Bioprinting Human Chondrocytes with Nanocellulose–Alginate Bioink for Cartilage Tissue Engineering Applications. *Biomacromolecules,* 16(5), 1489-1496.

Martínez Ávila, H., Feldmann, E.-M., Pleumeekers, M. M., Nimeskern, L., Kuo, W., de Jong, W. C., . . . Gatenholm, P. (2015). Novel bilayer bacterial nanocellulose scaffold supports neocartilage formation in vitro and in vivo. *Biomaterials,* 44, 122-133.

Matthews, I. P., Gibson, C., & Samuel, A. H. (1994). Sterilisation of implantable devices. *Clin Mater,* 15(3), 191-215.

Miao, Z., Lu, Z., Wu, H., Liu, H., Li, M., Lei, D., . . . Zhao, J. (2017). Collagen, agarose, alginate and Matrigel hydrogels as cell substrates for culture of chondrocytes in vitro: A comparative study. *J Cell Biochem*.

Möller, T., Amoroso, M., Hägg, D., Brantsing, C., Rotter, N., Apelgren, P., . . . Gatenholm, P. (2017). In Vivo Chondrogenesis in 3D Bioprinted Human Cell-laden Hydrogel Constructs. *Plastic and Reconstructive Surgery Global Open,* 5(2), e1227.

Mouser, V. H. M., Levato, R., Bonassar, L. J., D'Lima, D. D., Grande, D. A., Klein, T. J., . . . Malda, J. (2017). Three-Dimensional Bioprinting and Its Potential in the Field of Articular Cartilage Regeneration. *Cartilage,* 8(4), 327-340.

Müller, M., Öztürk, E., Arlov, Ø., Gatenholm, P., & Zenobi-Wong, M. (2016). Alginate Sulfate–Nanocellulose Bioinks for Cartilage Bioprinting Applications. *Annals of Biomedical Engineering*, 1-14.

Nava, M. M., Draghi, L., Giordano, C., & Pietrabissa, R. (2016). The effect of scaffold pore size in cartilage tissue engineering. *J Appl Biomater Funct Mater,* 14(3), e223-229.

Nguyen, D., Hagg, D. A., Forsman, A., Ekholm, J., Nimkingratana, P., Brantsing, C., . . . Simonsson, S. (2017). Cartilage Tissue Engineering by the 3D Bioprinting of iPS Cells in a Nanocellulose/Alginate Bioink. *Sci Rep,* 7(1), 658.

Oh, S. H., Kim, T. H., Im, G. I., & Lee, J. H. (2010). Investigation of pore size effect on chondrogenic differentiation of adipose stem cells using a pore size gradient scaffold. *Biomacromolecules,* 11(8), 1948-1955.

Paakko, M., Ankerfors, M., Kosonen, H., Nykanen, A., Ahola, S., Osterberg, M., . . . Lindstrom, T. (2007). Enzymatic hydrolysis combined with mechanical shearing and high-pressure homogenization for nanoscale cellulose fibrils and strong gels. *Biomacromolecules,* 8(6), 1934-1941.

Pan, Z., Duan, P., Liu, X., Wang, H., Cao, L., He, Y., . . . Ding, J. (2015). Effect of porosities of bilayered porous scaffolds on spontaneous osteochondral repair in cartilage tissue engineering. *Regen Biomater,* 2(1), 9-19.

Park, H., & Lee, K. Y. (2014). Cartilage regeneration using biodegradable oxidized alginate/hyaluronate hydrogels. *J Biomed Mater Res A,* 102(12), 4519-4525.

Peretz, S., Florea-Spirou, M., Anghel, D.-F., Bala, D., Stoian, C., & Zgherea, G. (2014). *Preparation of Porous Calcium Alginate Beads and Their Use for Adsorption of O-Nitrophenol from Aqueous Solutions*.

Revin, V., Liyaskina, E., Nazarkina, M., Bogatyreva, A., & Shchankin, M. (2018). Cost-effective production of bacterial cellulose using acidic food industry by-products. *Braz J Microbiol,* 49 Suppl 1, 151-159.

Rogers, W. J. (2012). *2 - Steam and dry heat sterilization of biomaterials and medical devices*. In S. Lerouge & A. Simmons (Eds.), *Sterilisation of Biomaterials and Medical Devices* (pp. 20-55): Woodhead Publishing

596 Skjåk-Bræk, G., Grasdalen, H., & Smidsrød, O. (1989). Inhomogeneous polysaccharide ionic gels. *Carbohydr Polym,*
597 10(1), 31-54.

598 Svensson, A., Nicklasson, E., Harrah, T., Panilaitis, B., Kaplan, D. L., Brittberg, M., & Gatenholm, P. (2005). Bacterial
599 cellulose as a potential scaffold for tissue engineering of cartilage. *Biomaterials,* 26(4), 419-431.

600 Tibbitt, M. W., & Anseth, K. S. (2009). Hydrogels as extracellular matrix mimics for 3D cell culture. *Biotechnol*
601 *Bioeng,* 103(4), 655-663.

602 Veerachamy, S., Yarlagadda, T., Manivasagam, G., & Yarlagadda, P. K. (2014). Bacterial adherence and biofilm
603 formation on medical implants: a review. *Proc Inst Mech Eng H,* 228(10), 1083-1099.

604 Villanueva, I., Klement, B. J., von Deutsch, D., & Bryant, S. J. (2009). Cross-linking density alters early metabolic
605 activities in chondrocytes encapsulated in poly(ethylene glycol) hydrogels and cultured in the rotating wall vessel.
606 *Biotechnol Bioeng,* 102(4), 1242-1250.

607 Wasikiewicz, J. M., Yoshii, F., Nagasawa, N., Wach, R. A., & Mitomo, H. (2005). Degradation of chitosan and sodium
608 alginate by gamma radiation, sonochemical and ultraviolet methods. *Radiation Physics and Chemistry,* 73(5), 287-295.

609 Xiao, Y., Friis, E. A., Gehrke, S. H., & Detamore, M. S. (2013). Mechanical testing of hydrogels in cartilage tissue
610 engineering: beyond the compressive modulus. *Tissue Eng Part B Rev,* 19(5), 403-412.

611 Yang, H., Yan, R., Chen, H., Lee, D. H., & Zheng, C. (2007). Characteristics of hemicellulose, cellulose and lignin
612 pyrolysis. *Fuel,* 86(12), 1781-1788.

613